PHYTOTHERAPY RESEARCH
Phytother. Res. **27**: 1819–1828 (2013)
Published online 17 February 2013 in Wiley Online Library
(wileyonlinelibrary.com) **DOI**: 10.1002/ptr.4939

A Biochemical and Cellular Approach to Explore the Antiproliferative and Prodifferentiative Activity of Aloe Arborescens Leaf Extract

Blanda Di Luccia,[1] Nicola Manzo,[1] Maria Vivo,[1] Eugenio Galano,[2] Angela Amoresano,[2] Elvira Crescenzi,[4] Alessandra Pollice,[1]* Raffaella Tudisco,[3] Federico Infascelli[3] and Viola Calabrò[1]

[1]Dipartimento di Biologia Strutturale e Funzionale, Università di Napoli 'Federico II', Naples, Italy
[2]Dipartimento di Chimica Organica e Biochimica, Università di Napoli 'Federico II', Naples, Italy
[3]Dipartimento di Scienze Zootecniche e Ispezione degli Alimenti, Università di Napoli 'Federico II', Naples, Italy
[4]Istituto di Endocrinologia ed Oncologia Sperimentale, CNR, via S. Pansini, 580131, Naples, Italy

***Aloe arborescens Miller*, belonging to the Aloe genus (Liliaceae family), is one of the main varieties of Aloe used worldwide. Although less characterized than the commonest *Aloe vera*, *Aloe arborescens* is known to be richer in beneficial phytotherapeutic, anticancer, and radio-protective properties. It is commonly used as a pharmaceutical ingredient for its effect in burn treatment and ability to increase skin wound healing properties. However, very few studies have addressed the biological effects of *Aloe* at molecular level. The aim of the research is to provide evidences for the antiproliferative properties of *Aloe arborescens* crude leaf extract using an integrated proteomic and cellular biological approach. We analysed the composition of an *Aloe arborescens* leaf extract by gas chromatography-mass spectrometry analysis. We found it rich in Aloe-emodin, a hydroxylanthraquinone with known antitumoral activity and in several compounds with anti-oxidant properties. Accordingly, we show that the *Aloe* extract has antiproliferative effects on several human transformed cell lines and exhibits prodifferentiative effects on both primary and immortalized human keratinocyte. Proteomic analysis of whole cell extracts revealed the presence of proteins with a strong antiproliferative and antimicrobial activity specifically induced in human keratinocytes by *Aloe* treatment supporting its application as a therapeutical agent. Copyright © 2013 John Wiley & Sons, Ltd.**

Keywords: Aloe arborescence; differentiation; proliferation.

Supporting information may be found in the online version of this article (Supplementary Material)

INTRODUCTION

Plants and their extracts are appreciated for their specific aroma, nutraceutical, and therapeutical properties, such as antimicrobial, antiproliferative, anti-inflammatory, immunostimulant, and antioxidative (Greathead, 2003). *Aloe arborescens Miller*, belonging to the Aloe genus (Liliaceae family), is one of the main varieties of Aloe used worldwide. It is commercially grown in South America (Brazil and Uruguay), South Africa and some Asian countries. The concentrated active extract from *Aloe arborescens* shares some therapeutical properties with the well-known and studied *Aloe vera* and is commonly used in medicinal applications to treat burn wounds and help accelerating the healing process of the skin. Recent studies have demonstrated that *Aloe arborescens* has immunostimulating activity in animal trials (Infascelli *et al.*, 2010), and it was found to have beneficial phytotherapeutic and anticancer properties (Lissoni *et al.*, 2009). It is known that the anticancer properties of *Aloe arborescens* depend not only on its immuno-modulatory effect, but also on a direct inhibition of cancer cell proliferation (Bedini *et al.*, 2009). Immunostimulatory effects are due to acemannan, while antiproliferative effects have been ascribed to anthracenic, antraquinonic, and aloenin-like compounds (Lissoni *et al.*, 2009). *Aloe arborescens* is also known for its effective burn treatment and ability to increase skin wound healing properties. Furthermore, it has been shown to be useful in reducing microbial growth and to kill a broad range of viruses and fungi, thereby providing extraordinary support for the gastrointestinal tract, mucous membranes, and connective tissue (Falcetti A., personal communications).

To determine the therapeutic effects of *Aloe arborescens*, a considerable number of clinical investigations have been done; however, very few studies have addressed the biological effects of *Aloe* at molecular level. The aim of the present study is to analyse the cellular response to treatment with *Aloe arborescens* crude leaf extract through a biochemical and cellular approach in order to support its application as a therapeutical agent.

MATERIALS AND METHODS

Preparation of the whole-leaf extract. Plants from Italian farms (Marsala, Sicily) certified for organic systems were cultivated in natural habitat and

* Correspondence to: Dr Alessandra Pollice, PhD. Dipartimento di Biologia Strutturale e Funzionale, Università di Napoli, 'Federico II', Via Cinzia, Monte S Angelo, 80126 Napoli, Italy.
E-mail: apollice@unina.it

Received 05 August 2012
Revised 26 November 2012
Accepted 09 January 2013

harvested when they were older than 4 years. The leaves were washed in tanks, laid in plastic bags, successively washed at 25°C and brushed in order to eliminate external impurity. After air drying, the leaves were submitted to a 'cold method' provided by HDR sas (Caserta, Italy) which allows to extract the active principles either from the inner part or from the cuticle. Commercial preparation of *Aloe* extract was stabilized by potassium sorbate and citric acid. Successively, the extract was stored in stainless still containers which were sealed to avoid air contact.

Cell culture and Aloe arborescens treatment. NHEK primary cells, derived from neonatal foreskin, were from Clonetics (San Diego, California).The HaCaT (human spontaneously immortalized keratinocyte) and MDA-MB231 (human breast adenocarcinoma) cell lines were maintained in Dulbecco's Modified Eagle's Medium (DMEM) supplemented with 10% fetal bovine serum and 1% penicillin-streptomycin. The keratinocyte-derived squamous carcinoma cell lines (SCC011 and SCC012) were previously described (Lefort *et al.*, 2007). The A431 (human epidermoid carcinoma) cell line was maintained in RPMI 1640 supplemented with 10% fetal bovine serum and 1% penicillin-streptomycin. All cell lines were cultured at 37°C in humidified atmosphere of 5% CO_2. Aliquots of *Aloe arborescens* fresh leaf extract were centrifuged at 10000 rpm for 10 min and sterilized using disposable Millex syringe filter units, pore size 0.22 μm (Millipore). Sterile extract was employed for the treatment at 10, 20, and 50% v/v, as indicated, in cell culture medium. Equal amounts of Aloe preservation medium were added to control samples. *Aloe*-treated and untreated cells were photographed and harvested for Western-blot analysis as described below.

Cell growth analysis. HaCaT spontaneously immortalized human keratinocytes, MDA-MB231 metastatic breast adenocarcinoma, A431 human epidermoid carcinoma, CaCo2 human epithelial colorectal adenocarcinoma cells, SCC011, and SCC022 squamous cell carcinoma (SCC) were plated in 35 mm dishes, at a cell density of 1×10^5 cells/plate. Cells were cultured in complete growth media supplemented or not with aliquots of fresh *Aloe arborescence* extract (10% v/v) for 6, 24, 30, 48, and 54 h collected, and counted in a Burker chamber. Cell extracts from treated and untreated cells were prepared and subjected to SDS-PAGE and immunoblot for gene-expression analysis.

Flow cytometry analysis. After treatments, cells were washed twice with phosphate-buffered saline (PBS) and harvested with 0.05% trypsin in 0.15% Na_2EDTA. Cells were then centrifuged, washed in PBS, fixed with ice-cold 70% ethanol, and stored overnight at 4°C. Fixed cells were washed in PBS and then incubated with propidium iodide (50 μg/ml) and RNAse A (10 μg/ml) for 30 min at room temperature. Data acquisition was performed using a CyAn ADP Flow Cytometer (Beckman Coulter, Inc., Milano, Italy) and Summit Software.

Keratinocyte differentiation. Non tumorigenic HaCaT cells were chosen because they retain the ability to differentiate upon Ca2+ treatment thus representing an intermediary between normal and cancerous keratinocytes. HaCaT cells were grown to confluence in complete growth medium and switched into differentiation medium (serum-free DMEM) with 1.2 mM $CaCl_2$ with or without *Aloe extract* (10% v/v) for 6 days according to (Vivo *et al.*, 2009), with the exception that the medium was changed every 48 h. Differentiated cells treated or not with *Aloe* were photographed and harvested for SDS-PAGE and immunoblot analysis as described below. NHEK cells were propagated in serum-free keratinocyte growth medium containing 0.05 mM calcium. NHEK cells with 70%–80% cell confluency were switched to high-calcium medium (1.2 mM) to induce differentiation. Extracts from *Aloe*-treated or untreated NHEK cells were then subjected to SDS-PAGE and immunoblot analysis as described below.

SDS-PAGE and immunoblot analysis. *Aloe arborescens* treated and untreated cells were harvested in lysis buffer (50 mM Tris–HCl pH 7.5, 5 mM EDTA, 150 mM NaCl, 1% NP-40, 1 mM phenylmethylsulfonyl fluoride, 0.5% sodium deoxycholate, and protease inhibitors). Cell lysates were incubated on ice for 40 min, and the extracts were centrifuged at 13200 rpm for 15 min to remove cell debris. Protein concentrations were determined by the Bio-Rad protein assay (Bio-Rad). After the addition of 2× Laemmli buffer (SIGMA), the samples were boiled at 100°C for 5 min and resolved by SDS-polyacrylamide gel electrophoresis. Proteins were transferred to a polyvinylidene difluoride membrane (Millipore). The PVDF membrane was blocked in 5% w/v milk buffer (5% w/v non-fat dried milk, 50 mM Tris, 200 mM NaCl, 0,2% Tween 20) and incubated with primary antibodies diluted in 5% w/v milk or bovine serum albumine buffer for 2 h at room temperature or overnight at 4°C. Primary antibodies were anti-mouse p63-4A4 (Calbiochem), anti-mouse involucrin (Abcam antibody), anti-mouse cytokeratin 1 (Santa-Cruz biotechnology), anti-rabbit transglutaminase type 2 (Abcam antibody), anti-rabbit pErks 42/44 (Cell signalling), anti-rabbit p21 (Santa-Cruz biotechnology), anti-rabbit cyclin D1 (Cell Signalling), anti-rabbit PARP-1 (Cell Signalling), and anti-goat β-actin (Santa-Cruz biotechnology). Data were visualized by enhanced chemiluminescence method (GE-Healthcare) using HRP-conjugated secondary antibodies (Santa-Cruz biotechnology) incubated for 1 h at room temperature and analysed by Quantity One ®software of ChemiDoc ™XRS system (Bio-Rad).

Cell fluorescent staining. SCC011 and SCC022 cells were seeded on sterile coverslips and treated or not with Aloe arborescens extract (10% v/v) for 48 h. After the treatment, three washes with PBS were performed, and cells were fixed with 4% paraformaldehyde at RT for 15 min. Then, cells were incubated with Wheat Germ Agglutinin (WGA) membrane fluorescent stain (1:200) for 1 h at 37°C. After three washes with PBS, cells were permeabilized with 0.5% Triton-X100 (Sigma-Aldrich, Selze/Germany) at room temperature for 5 min. Following permeabilization, cells were incubated with DAPI (1:10000) for 3 min at RT. After three washes with 0.05% PBS-Tween, slides were mounted and analysed.

Metabolite analysis. Aliquots of commercial preparation of aloe extract were submitted to liquid–liquid extraction procedure by using equal amount of chloroform (1:1 v/v). The extraction step was performed three times, and the

organic extracts were collected and dried. Analyte mixtures were finally trimethylsilylated in 200 µl of N, O-bis(trimethylsilyl) acetamide at 80°C for 45 min. The sample was dried down under nitrogen, dissolved in 50 µl of hexane, and centrifuged to remove the excess of solid reagents. The hexane supernatant (1/50) was used for the gas chromatography-mass spectrometry (GC-MS) analysis.

GC-MS analysis. GC-MS analyses were performed on a 5390 MSD quadrupole mass spectrometer (Agilent technologies) equipped with a gas chromatograph by using a DB-5MS fused silica capillary column (30 m, 0.5 mm ID, 0.25 µm ft) from G&W. The injection temperature was 250°C. For lipid analyses, the oven temperature was increased from 25°C to 90°C in 1 min and held at 90°C for 1 min before increasing to 140°C at 25°C/min, to 200°C at 5°C/min and finally to 300°C at 10°C/min. Electron Ionization mass spectra were recorded by continuous quadrupole scanning at 70eV ionization energy. Each species was interpreted on the basis of electron impact spectra (NIST library and Analyst Software).

Two-dimensional electrophoresis (2DE). The first dimensional electrophoresis (isoelectric focusing, IEF) was carried out on non-linear wide-range immobilized pH gradients (pH 4–7; 7 cm long IPG strips; GE Healthcare, Uppsala, Sweden) and achieved using the Ettan IPGphor system (GE Healthcare, Uppsala, Sweden). 200 µg of protein extracts was precipitated with methanol/chloroform according to (Wessel and Flugge, 1984) and solubilized in 125 µl of rehydratation buffer and 0.2% (v/v) carrier ampholyte for 12 h, at 50 mA, at 20°C. The strips were then focused according to the following electrical conditions at 20°C: 500 V for 30 min, 1000 V for 30 min, 5000 V for 10h, until a total of 15000 Vt was reached. After focusing, analytical and preparative IPG strips were equilibrated for 15 min in 6 M urea, 30% (V/V) glycerol, 2% (w/V) SDS, 0.05 M Tris–HCl, pH 6.8, 1% (w/V) dithiothreitol (DTT), and subsequently for 15 min in the same urea/SDS/Tris buffer solution but substituting the 1% (w/V) DTT with 2.5% (w/V) iodoacetamide. The second dimension was carried out on 12.5% (w/w) polyacrylamide gels (10 cm × 8 cm × 0.75 mm) at 25 mA/gel constant current and 10°C until the dye front reached the bottom of the gel, according to (Laemmli, 1970; Hochstrasser *et al.*, 1988). MS-preparative gels were stained overnight with colloidal Coomassie Brilliant Blue and destained with MilliQ grade water.

Image analysis. Gels images were acquired with an Epson expression 1680 PRO scanner. Computer-aided 2-D image analysis was carried out using the ImageMasterTM 2D Platinum software. Relative spot volumes (%V) (V = integration of OD over the spot area; %V = V single spot/V total spot) were used for quantitative analysis in order to decrease experimental errors.

In situ digestion. Trypsin, DTT, iodoacetamide, and R-cyano-4-hydroxycinnamic acid were purchased from Sigma. NH4HCO3 was from Fluka. Trifluoroacetic acid-high-performance liquid chromatography (HPLC) grade was from Carlo Erba. All other reagents and solvents were of the highest purity available from Baker. Analysis was performed on the Coomassie blue-stained spots excised from the gels. The spots were excised from the gel and destained by repetitive washes with 0.1 M NH4HCO3, pH 7.5, and acetonitrile. Samples were reduced by incubation with 50 µl of 10 mM DTT in 0.1 M NH4HCO3 buffer, pH 7.5 and carboxyamidomethylated with 50 µl of 55 mM iodoacetamide in the same buffer. Enzymatic digestion was carried out with trypsin (12.5 ng/µl) in 10 mM ammonium bicarbonate buffer, pH 7.8. Gel pieces were incubated at 4°C for 2 h. Trypsin solution was then removed, and a new aliquot of the same solution was added; samples were incubated for 16 h at 37°C. A minimum reaction volume was used as to obtain the complete rehydration of the gel. Peptides were then extracted by washing the gel particles with 10 mM ammonium bicarbonate and 1% formic acid in 50% acetonitrile at room temperature. The resulting peptide mixtures were filtrated using 0.22 PDVF filter from Millipore, following the recommended procedure.

NanoHPLC-chip MS/MS analysis. The peptide mixtures were analysed using a CHIP MS 6520 QTOF equipped with a capillary 1200 HPLC system and a chip cube (Agilent Technologies, Palo Alto, Ca). After loading, the peptide mixture (8 µl in 0.1% formic acid) was first concentrated and washed at 4 µl min^{-1} in 40 nl enrichment column (Agilent Technologies chip), with 0.1% formic acid in 2% acetonitrile as eluent. The sample was then fractionated on a C18 reverse-phase capillary column (75 µm × 43 mm in the Agilent Technologies chip) at flow rate of 400 nl min^{-1} with a linear gradient of eluent B (0.1% formic acid in 95% acetonitrile) in A (0.1% formic acid in 2% acetonitrile) from 7 to 60% in 50 min.

Peptide analysis was performed using data-dependent acquisition of one MS scan (mass range from 400 to 2000 m/z) followed by MS/MS scans of the three most abundant ions in each MS scan. The acquired MS/MS spectra were transformed in Mascot generic file format and used for peptides identification with a licensed version of MASCOT 2.1, in a local database (Swiss Pro).

Protein identification. Raw data from nano-LC–MS/MS were analysed using Qualitative Analysis software, and MSMS spectra were searched against non-redundant protein databases (NCBInr 20090924, 9760158 sequences) and UniprotSwissprot (2011, 167910 sequences), with the taxonomy restriction to Homo sapiens, using in-house MASCOT 2.1 software (Matrix Science, Boston, USA).

The Mascot search parameters were: 'trypsin' as enzyme allowing up to three missed cleavages, carbamidomethyl on as fixed modification, oxidation of M, pyroGlu N-term Q, as variable modifications, 20 ppm MSMS tolerance, and 0.6 Da peptide tolerance. The score used to evaluate quality of matches for MSMS data was higher than 32.

Phase-contrast microscopy. HaCaT and A431 cells were grown and (HaCaT) induced to differentiate on glass coverslips in six-well plates, washed with PBS and fixed with cold methanol for 10 min. Treated and not-treated cells were photographed (40×) with Olympus BX51 microscope.

Bacterial strains and growth conditions. Bacterial strains used in this study were *Bacillus cereus* (*6A2*) (Naclerio *et al.*, 1993), *Staphylococcus aureus* (ATCC 6538), *Listeria monocitogenes* (ATCC 7644), *Salmonella typhimurium*

(ATCC 14028), *Shigella sonnei* (ATCC25931), *Escherichia coli* (DH5α), *Bacillus subtilis* (PY79) (Youngman *et al*., 1984), *Lactobacillus mucosae* (SF1031), and *Lactobacillus gasseri* (SF1109) (Fakhry *et al*., 2009). Lactobacilli cultures were cultured in MRS broth (Difco) at 37°C in microaerophilic conditions, while for all other strains, LB medium (8 g/l NaCl, 10 g/l tryptone, 5 g/l yeast extract) and aerobic conditions at 37°C were used. *Aloe*-containing liquid media, obtained by adding 2 ml of an aqueous *Aloe* leaf extract to 8 ml of LB or MRS media, were inoculated with 0.1 ml of an overnight culture and growth at 37°C followed for 8-12 h by spectrophotometer (OD_{600}) analysis.

Plate antibacterial assays. For each indicator strain utilized, 100 µl aliquots of exponential growth cultures was mixed with 10 ml of LB or MRS soft agar (0.7%). Plates were then spotted with 10 µl of *Aloe arborescens* extract, incubated at 37°C and the inhibition halo measured as previously reported (Baccigalupi *et al*., 2005). The effects of *Aloe arborescens* extracts on bacterial growth were also measured on LB and MRS agar plates prepared by adding various dilutions of *Aloe* extract (1:1, 1:5, 1:10) to the media and then spotting on the solidified plates aliquots (10 µl) of each bacterial culture in stationary growth phase. *Aloe*-containing plates were then incubated 37°C and checked for bacterial growth after 24 and 48 h.

RESULTS AND DISCUSSION

GC-MS analysis

The composition of the *Aloe arborescens* preparation was determined by GC-MS analyses following liquid–liquid extraction of different analytes from the extract. The extracted mixture of species was derivatized to TMS derivatives and directly analysed by GC-MS by monitoring the total ion current as a function of time. Each species was univocally identified on the basis of the electron impact fragmentation spectra. All the analyses were performed as triplicates. The chromatograms of organic phase extracted in chloroform essentially revealed the presence of hesenoic (C6H12O2), sorbic (C6H8O2), and benzoic acid (C6H8O7). In the aqueous phase, 22 predominant species were identified and are listed in Table 1. Aloin, one of the main component of Aloe species with known pharmacological activities, was not detected, while a significant amount of Aloe-emodin, a hydroxylanthraquinone having specific antineuroectodermal tumor activity (Pecere *et al*., 2000), was present (14%).

Aloe arborescens affects cancer cell proliferation

It is already known that *Aloe arborescens* has antiproliferative and anticancer effects (Lissoni *et al*., 2009; Bedini *et al*., 2009); however, the molecular mechanisms underlying the cellular response to *Aloe* treatment remains to be defined. This prompted us to analyse the effect of an *Aloe arborescens* leaf extract on cell proliferation at cellular and molecular level, by comparing the rate of cell proliferation, the cell-cycle distribution, and the expression of cell-cycle-related molecular markers in *Aloe*-treated and untreated human cells. These analyses were performed in A431 (epidermoid skin carcinoma), MDA-MB231 (metastatic breast cancer), CaCo-2 (epithelial colorectal adenocarcinoma), and HaCaT spontaneously immortalized keratinocytes. As shown in Fig. 1, we reproducibly

Table 1. List of species identified by GC-MS in the *Aloe arborescens* commercial preparation. The relative abundance is expressed as percentage of total volume injected. Preservatives are indicated in bold.

Peak N°	Retention time (min)	Compound	Molecular formula	% of total
1	**4.28**	**Sorbic acid**	**$C_6H_8O_2$**	**3.88**
2	5.00	Benzoic acid	$C_7H_6O_2$	10.95
3	5.16	Phosphoric acid	H_3PO_4	9.27
4	5.76	Succinic acid	$C_4H_6O_4$	11.67
5	6.17	Itaconic acid	$C_5H_6O_4$	0.27
6	7.54	Octanoic acid	$C_8H_{16}O_2$	0.10
7	8.68	Malic acid	$C_4H_6O_5$	0.06
8	9.19	4-hydroxycyclohexylcarboxylic acid	$C_7H_{12}O_3$	1.76
9	10.08	Rythronic acid	$C_{16}H_{40}O_5Si_4$	0.08
10	10.58	α-hydroxycinnamic acid	$C_9H_{10}O_3$	0.11
11	12.01	Pimelic acid	$C_7H_{12}O_4$	0.35
12	13.17	Isocitric acid lactone	$C_6H_6O_6$	0.39
13	13.50	Cyclooctene-1,2-diol	$C_8H_{14}O_2$	0.21
14	13.71	Tricarballylic acid	C_6H_8O6	0.96
15	14.21	para-Coumaric acid	$C_9H_8O_3$	0.38
16	14.72	Terephtalic acid	$C_8H_6O_4$	0.08
17	**15.27**	**Citric acid**	**$C_6H_8O_7$**	**44.74**
18	16.37	Ferulic acid	$C_{10}H_{10}O_4$	0.15
19	17.11	2,4,6-tri-tert-butylphenol	$C_{18}H_{30}O$	0.24
20	18.34	Palmitic acid	$C_{16}H_{32}O_2$	0.10
21	19.92	1H-Indole-2,3-dione-6-ethoxy	$C_{22}H_{22}N_2O_5$	0.08
22	22.26	1,8-Dihydroxy-3-(hydroxymethyl)-9,10-anthracenedione (Aloe-emodin)	$C_{15}H_{10}O_5$	14.01

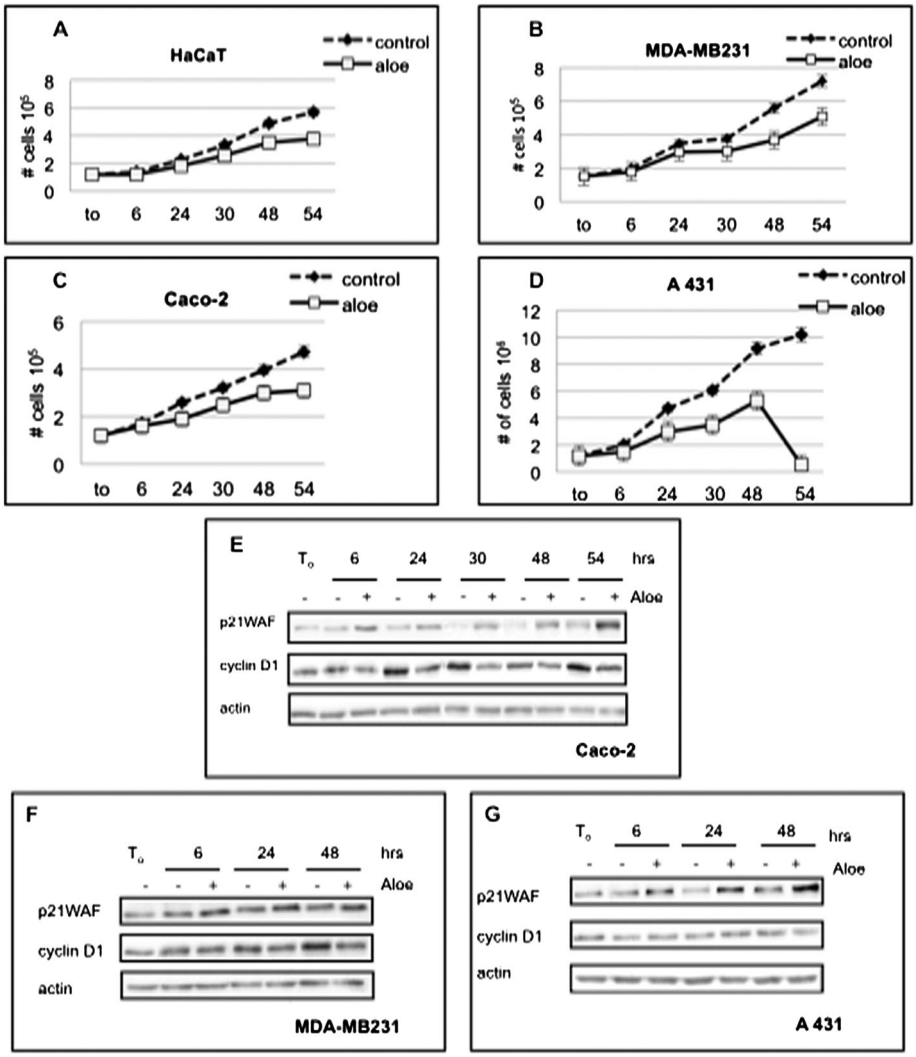

Figure 1. (A) Proliferating HaCaT, (B) MDA-MB231, (C) CaCo-2, (D) A431 cells were incubated in complete cell culture medium supplemented or not with *Aloe* extract (1:10 v/v). Control and *Aloe*-treated cells were collected at 6, 24, 30, 48, and 54 h and counted in a Burker chamber. (E) 'Proliferating CaCo-2, (F) MDA-231, (G) A431 cells were incubated in complete cell culture medium supplemented or not with *Aloe* extract (1:10 v/v). Control and *Aloe*-treated cells were harvested at indicated different times (h). Equal amount of cell lysates was subjected to immunoblot analysis with antibodies against cyclin D1 and p21WAF. Actin was used as a loading control.

found that *Aloe* extract reduces the cell proliferation rate in all cell lines tested. At 54 h of exposure to *Aloe*, a 30 to 40% reduction in the number of cells was observed in MDA-MB231, CaCo2, and HaCaT cells, while A431 cells stopped to proliferate and underwent a drastic massive cell death (Fig. 1D). The cell-cycle distribution of control and *Aloe*-treated cells by flow cytometry shows that HaCaT cells display only a slight increase (3%) in the percentage of G2/M cells after 48 h of *Aloe* treatment (Fig. 2), while the other cell lines tested display an increase of cells in S and/or G2/M phase with a compensatory decrease of G0/G1 phase population indicating that cells were unable to resume the cell cycle at normal phase transit rate. Moreover, except for HaCaT keratinocytes, *Aloe* treatment also caused a significant increase in sub-G1 cell population.

Expression of the cell-cycle markers p21WAF and Cyclin D1 was also investigated to explore *Aloe* effect at the molecular level. Immunoblots with the appropriate antibodies show that *Aloe* treatment significantly induced p21WAF in all tumor cells tested, while Cyclin D1 expression was inhibited in CaCo-2 and MDA-MB231 cells (Fig. 1E and F). Cyclin D1 is a labile factor required at high level for progression through the G1 phase of the cell cycle. Mitogenic pathways directly up-regulate the expression of Cyclin D1; therefore, impaired induction of Cyclin D1 with the concomitant increase of p21WAF is perfectly in line with the ineffectiveness of *Aloe*-treated cells to efficiently resume the cell cycle. Unexpectedly, A431 cells seemed to be unable to regulate Cyclin D1 expression (Fig. 1G). We can speculate that the delay or failure of Cyclin D1 induction with the concomitant increase of p21WAF might be responsible, at least in part, for the massive A431 cell detachment at 54 h of Aloe treatment. Importantly, although we observed an increase of sub-G1 cells upon *Aloe* treatment (Fig. 2), we were unable to observe PARP-1 cleavage by western blot analyses (see Supplementary Fig. 1a) thereby indicating that *Aloe* treatment was not inducing apoptosis. Annexin V assay confirmed the result (see Supplementary Fig.1b).

Aloe arborescens induces keratinocyte differentiation

The concentrated leaf extract from *Aloe arborescens* plants has been used for hundreds of years in medicinal applications to help accelerating the healing process of

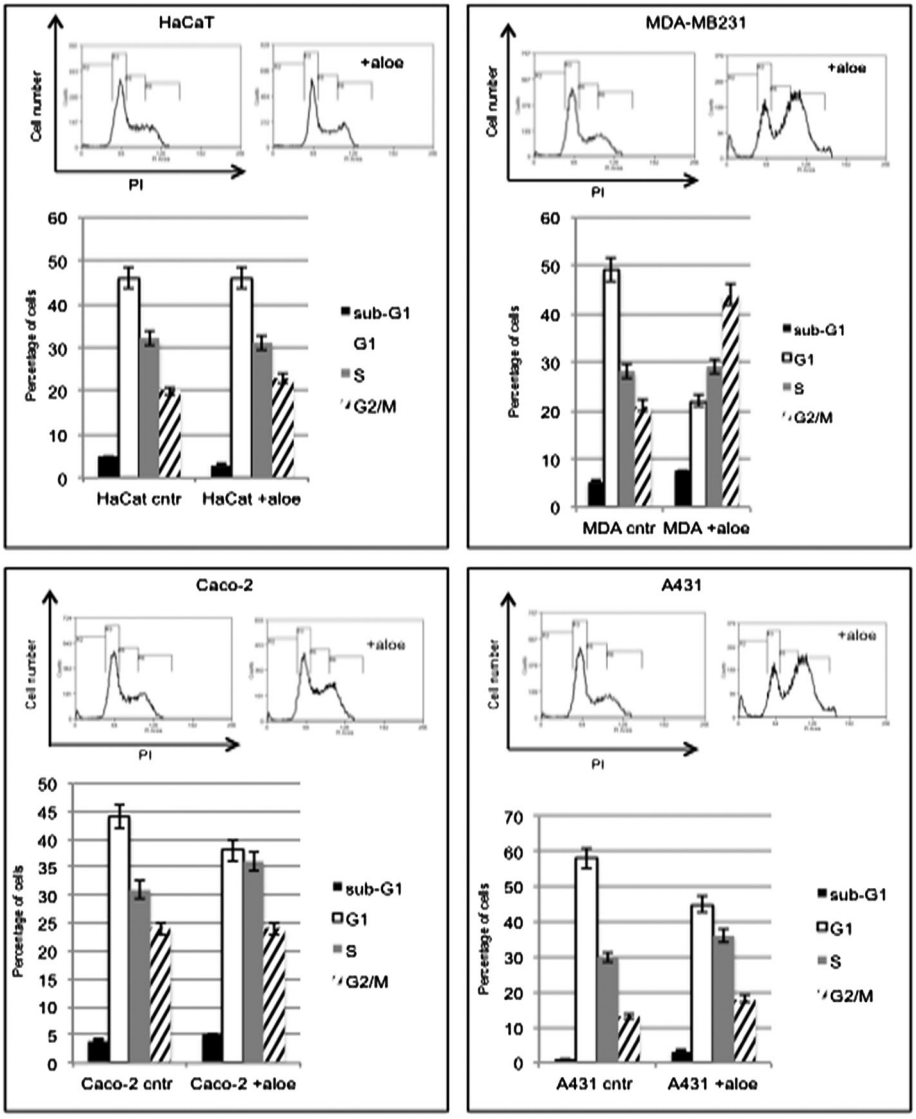

Figure 2. Representative data obtained from flow-cytometric analysis of cell cycle of HaCat, MDA-MB231, CaCo-2, and A-431cells incubated with or without *Aloe* for 48 h.

the skin. Therefore, we decided to analyse the effect of *Aloe arborescens* on differentiation of human keratinocytes. We decided to compare the behavior of HaCaT cells (spontaneously immortalized human keratinocytes) that retain the ability to differentiate upon Ca^{2+} treatment with that of human primary keratinocytes. Addition of calcium to keratinocyte cultures is the most physiological stimulus to elicit a rather complete differentiation program, inducing not only biochemical markers but also many of the structural changes occurring *in vivo* (Dotto, 1999). To check whether the differentiation profile is altered by *Aloe* treatment, HaCaT cells were induced to terminally differentiate by adding 1.2 mM calcium in a serum-free medium, supplemented or not with *Aloe* extract. After 6 days of culture, *Aloe*-treated cells became shrunken and pluristratified (Fig. 3A). To provide molecular evidence that differentiation was anticipated by *Aloe* treatment, we performed immunoblot analyses on extracts derived from treated and untreated cells. In particular, we observed that Involucrin and Transglutaminase, two well-characterized differentiation markers (Paramio and Jorcano, 1997), were expressed at higher levels in *Aloe*-treated cells. Conversely, ΔNp63α that is associated with the proliferative potential of epithelial cells and disappears in terminally differentiated keratinocytes (Di Costanzo *et al.*, 2009) was down-regulated earlier upon *Aloe* treatment (Fig. 3B).

In human primary keratinocytes (NHEK), *Aloe* treatment caused a dramatic increase of Involucrin gene expression that was already evident after 1 day of treatment. Similar to what we have observed in HaCaT cells, ΔNp63α level decreased faster in *Aloe*-treated keratinocytes compared with control cells (Fig. 3C).

We then looked more deeply into the effect of *Aloe* treatment during the early phases of HaCaT cell differentiation. To this purpose, HaCaT cells were seeded at medium density (2.5×10^5) in complete medium supplemented or not with *Aloe* extract (1:10 v/v) and collected before *Aloe* addition (t0) or after 6, 24, 30, 48, and 54 h after *Aloe* treatment (Fig. 3D). Equal amounts of cell lysates were subjected to immunoblot analysis to detect endogenous p21WAF and Cyclin D1. ΔNp63α and Cytokeratin 1 (CK1) were also monitored as early differentiation markers. As shown in Fig. 3D, we initially observed an increase of Cyclin D1 protein levels both in *Aloe*-treated and untreated keratinocytes. However,

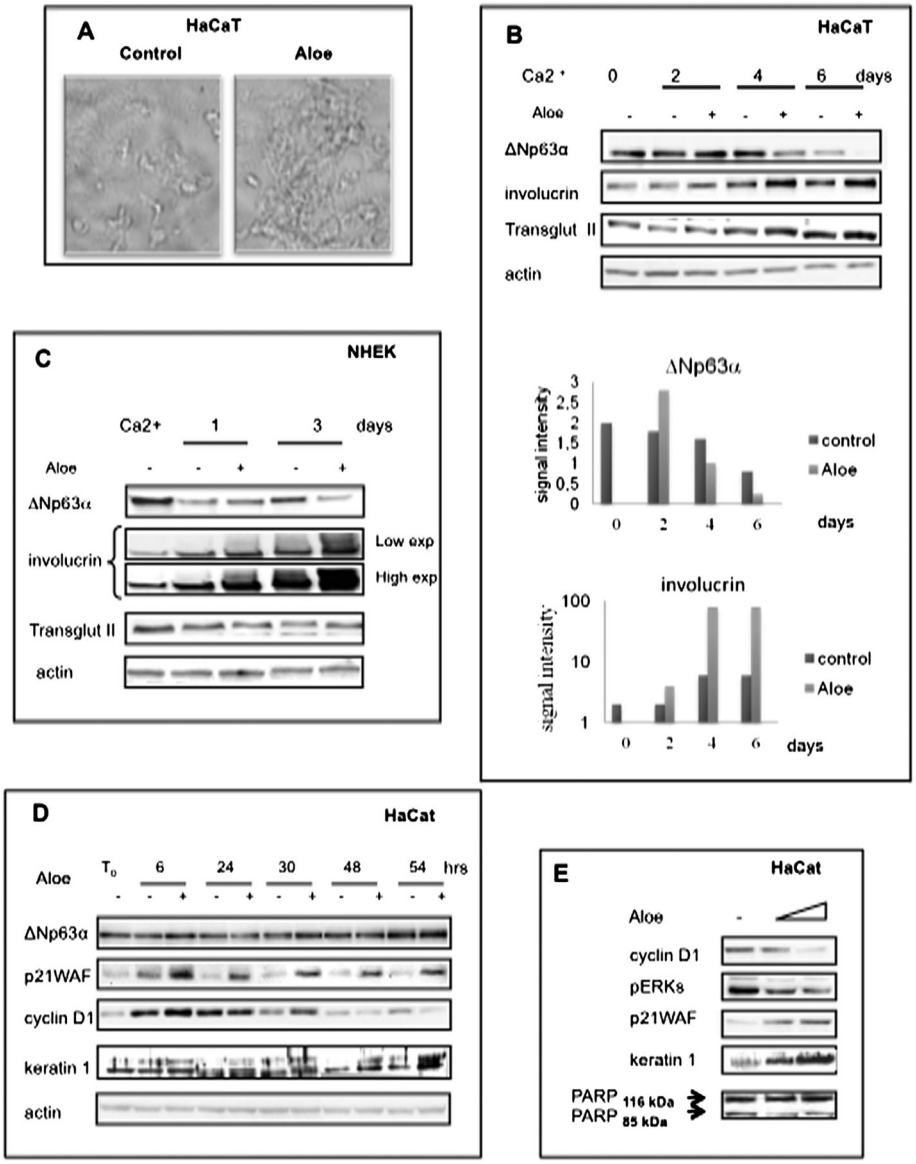

Figure 3. (A) Confluent HaCaT cells were induced to terminally differentiate by serum withdrawal and calcium addition (1,2 mM) in DMEM cell culture media supplemented or not with Aloe extract (1:10 v/v). After 6 days of culture, treated and non-treated cells were fixed with cold methanol and analysed by phase-contrast microscopy. (B) Differentiated HaCaT and (C) NHEK cells in presence or absence of *Aloe* extract (1:10 v/v) were collected at different indicated times. Equal amount of cell lysates was subjected to immunoblot analysis with antibodies against ΔNp63α, involucrin, and transglutaminase type II. Actin was used as a loading control. (D) Proliferating HaCaT cells were incubated in DMEM or DMEM *Aloe* extract containing medium (1:10 v/v). Control and *Aloe*-treated cells were collected at 6, 24, 30, 48, and 54 h. Equal amount of cell lysates was subjected to immunoblot analysis with antibodies against ΔNp63α, cyclin D1, p21WAF, and Keratin 1, an early differentiation marker. Actin was used as a loading control. (E) Proliferating HaCaT cells were incubated in DMEM or DMEM *Aloe* extract containing medium (20% or 50% v/v). Control and Aloe-treated cells were collected at 24 h. Equal amount of cell lysates were subjected to immunoblot analysis with antibodies against cyclin D1, p21WAF, Keratin 1, an early differentiation marker, and PARP-1. Actin was used as a loading control.

according to what observed in tumor cells, Cyclin D1 tended to be down-regulated faster in *Aloe*-treated HaCaT cells while the p21WAF protein was up-regulated only in *Aloe*-treated cells. At 54 h of *Aloe* treatment, the remarkable decrease of Cyclin D1 along with sustained expression of p21WAF indicates that keratinocytes were anticipating cell-cycle withdrawal. p21WAF-depleted keratinocytes exhibit an increased proliferative potential and a drastic down-modulation of keratinocyte differentiation markers (Di Cunto *et al.*, 1998) pointing to an essential involvement of p21WAF in the control of keratinocyte terminal differentiation. In line with these observations, compared to control cells, *Aloe*-treated keratinocytes exhibited higher levels of p21WAF and CK1, in agreement with the induction of a differentiation program. However, the persistence of ΔNp63α protein expression indicates that both treated and untreated keratinocytes were not fully differentiated (Fig. 3D).

Cyclin D1 protein is known to increase under mitogenic signals, through activation of the ERK's pathway. Remarkably, immunoblot analysis of lysates from proliferating HaCaT keratinocytes treated for 24 h with increasing amounts of *Aloe arborescens* extract (20% or 50% v/v) show that the reduction of Cyclin D1 and phosphorylated ERKs, as well as the induction of p21WAF and CK1, was dose dependent. Moreover, the signal corresponding to the cleavage of PARP1 was not enhanced, thus indicating that cells were not undergoing apoptosis (Fig. 3E).

We then decided to look at the effect of *Aloe* treatment on squamous carcinoma cell lines (SCC011 and SCC022). SCC is an uncontrolled growth of abnormal cells arising in the squamous layer, which composes most of the skin's upper layers. SCC cells retain high levels of ΔNp63α that is absolutely required for the survival of early stages of the squamous carcinoma. We first determined the rate of cell proliferation in control and *Aloe*-treated SCC011 and SCC022 cells. As shown in Fig. 4A and B, in *Aloe* containing medium, both SCC011 and SCC022 cells stop growing. The cell-cycle profile of *Aloe*-treated SCC022 cells reveals a dramatic increase in percentage of sub-G1 cells at the expenses of G1 and G2/M cells (Fig. 4C). In SCC011, the increase of subG1 cells was less dramatic although the S phase arrest was evident (Fig. 4D). Growth arrest was associated with a characteristic enlarged and flattened cell morphology as shown by fluorescence microscopy in SCC011 cells (Fig. 4E). Interestingly, compared to SCC022, SCC011 cells display a stronger activation of the Akt survival marker (data not shown) suggesting that Akt may, indeed, counteract *Aloe*-induced cell death. Western blot analysis of control and *Aloe*-treated SCC011 shows a dramatic decrease of ΔNp63α and a concomitant increase of p21WAF and CK1 polymers (Fig. 4F). Importantly, since it has been shown that SCC011 and SCC022 proliferation is strictly dependent on ΔNp63α (Rocco *et al*., 2006), the dramatic reduction of ΔNp63α induced by *Aloe* in these tumor cells may account for the cell death observed

Antibacterial tests

Inner leaf extract from *Aloe vera* was shown to inhibit growth of Streptococcus and Shigella species in vitro (Arunkumar and Muthuselvam, 2009). Aloe-emodin has been proposed to have direct antimicrobial activity. To assess whether the *Aloe* aqueous extract had antibacterial effects, two different plate antibacterial assays were performed with a panel of nine bacterial strains. As a first assay, LB or MRS plates were disseminated with each of the bacterial strain and spotted with the aliquots of *Aloe* extract. As a second assay, LB or MRS solid media containing various amounts of *Aloe* extract were spotted with aliquots of bacterial cells previously grown in liquid media. With both assays, no inhibition of bacterial growth was observed for any of the nine bacterial strains analysed (data not shown).

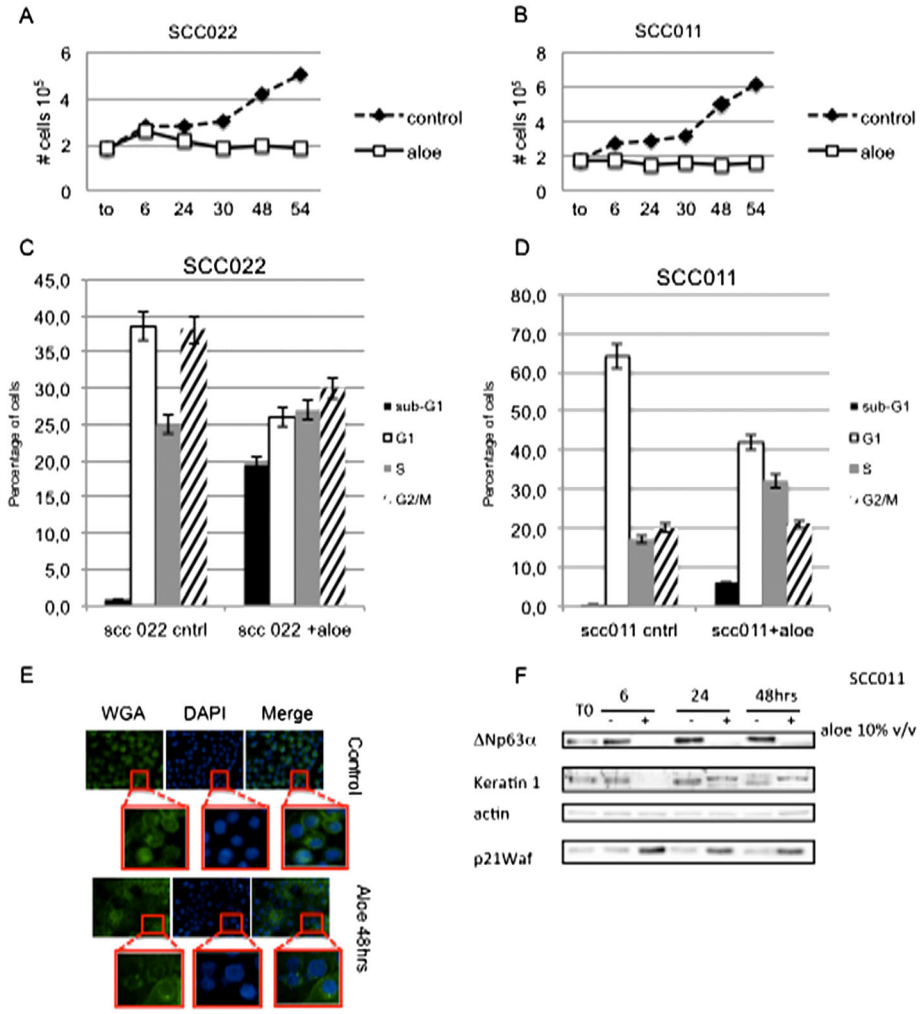

Figure 4. (A) Proliferating SCC022 and (B) SCC011 cells were incubated in complete cell culture medium supplemented or not with *Aloe* extract (1:10 v/v). Control and *Aloe*-treated cells were collected at 6, 24, 30, 48, and 54 h and counted in a Burker chamber. (C) and (D) Representative data obtained from flow-cytometric analysis of cell cycle of SCC022 and SCC011 cells incubated with or without *Aloe* for 48 h. (E) Representative images of SCC011 cells fluorescently stained with WGA (labeling membrane glycoproteins) or DAPI. (F) Equal amount of cell lysates was subjected to immunoblot analysis with indicated antibodies. Actin was used as a loading control. This figure is available in colour online at wileyonlinelibrary.com/journal/ptr.

Table 2. List of proteins differentially represented in *Aloe*-treated or control HaCaT cells identified by mass spectrometry.

Aloe-treated Spot	MW	Score	Protein	Swissprot code	Peptides	Sequence coverage
1	72402	186	**78 kDa glucose-regulated protein**	P11021	8	20%
2	50095	325	**Tubulin beta chain**	P07437	11	34%
3	11391	37	**Dermcidin**	P81605	3	30%
4	29843	60	**Prohibitin**	P35232	6	25%
5	22826	175	**Heat shock protein beta-1**	P04792	4	33%
6	22436	53	**UMP-CMP kinase**	P30085	4	42%
7	23569	47	**Glutathione S-transferase P**	P09211	6	42%
8	17292	60	**Stathmin**	P16949	2	18%
Control						
Spot	**MW**	**Score**	**Protein**	**Swissprot Code**	**Peptides**	**Sequence coverage**
9	62255	83	**Keratin, type I cytoskeletal 9**	P35527	5	10%
10	71082	224	**Heat shock cognate 71 kDa protein**	P11142	13	23%
11	73920	49	**Stress-70 protein, mitochondrial**	P38646	7	12%
12	70294	68	**Heat shock 70 kDa protein 1A/1B**	P08107	4	8%
13	61187	492	**60 kDa heat shock protein, mitochondrial**	P10809	24	50%
14	42052	156	**Actin, cytoplasmic 1**	P60709	9	34%
15	32726	267	**Nucleophosmin**	P06748	10	26%
16	27871	189	**14-3-3 protein sigma**	P31947	9	37%
17	16827	101	**Calmodulin**	P62158	2	29%

Proteomic analysis

Although *Aloe arborescens* extract has been largely used for its immunostimulating and anticancer properties, little is known of its impact at the proteome level. We thus decided to look at cell proteome changes of HaCaT keratinocytes induced by *Aloe* treatment. Protein extracts from untreated (Control) or *Aloe*-treated (Sample) HaCaT cells were fractionated by 2D-GE and stained with colloidal Blue Coomassie. The gels were run in triplicate and compared using the ImageMaster 2D Platinum 6.0 software. A few initial reference points (landmarks) were affixed for gels alignment in the first step of the images analysis. The spots were detected on the gels and the software 'matched' the gels and the corresponding spots. The spots representing the same protein in different gels were paired. Pairs were automatically determined using ImageMaster powerful gel matching algorithm. The different 2DE images were compared by synchronized 3-D spots view. Among the spots corresponding to *Aloe*-sensitive proteins clearly detected in repeated trials, 17 were selected for proteomic analysis. The image analysis enabled the identification of eight spots that were present either in higher amount or exclusively in the *Aloe*-treated sample, thereby indicating that they were induced by *Aloe* treatment. In the control sample, instead, nine spots that were undetectable or whose signal decreased after *Aloe* treatment were detected. These spots were selected for mass spectral identification by the merging of images analyses. Proteins excised from the gel were reduced, alkylated, and, in situ, digested with trypsin. The resulting peptide mixtures were analysed by nanoLC/MS/MS experiments. The peptide mixtures were fractionated by nanoHPLC and sequenced by MS/MS, generating sequence information on individual peptides. MSMS spectra were used to search for a non-redundant sequence using the in-house MASCOT software, thus taking advantage of the specificity of trypsin and of the taxonomic category of the samples. The number of measured masses that matched within the given mass accuracy was recorded, and the proteins that had the highest number of peptide matches were examined leading to the identification of the protein components. As further selection criteria, only the proteins, identified by MASCOT search with at least two peptides and found exclusively in the replicates, were selected. The list of proteins identified by this approach is illustrated in Table 2.

Among the identified proteins, a signal corresponding to **Tubulin** showed an increment in the treated sample as well as that of a powerful antimicrobial peptide known as **Dermcidin** (DCD). This observation was particularly intriguing as we failed to detect a direct antimicrobial activity of *Aloe arborescens* against several bacterial strains (see above). DCD is constitutively expressed in eccrine sweat glands and is part of the constitutive innate defence of human skin and stimulates keratinocytes to produce cytokines and chemokines (Niyonsaba *et al.*, 2009). So far, no DCD expression was found, neither at RNA nor at protein level, in primary keratinocytes, fibroblasts, and melanocytes both in normal conditions, or in cells stimulated by LPS, TNFα, or TPA. Although the *Aloe* ability to stimulate DCD production by keratinocytes needs further investigations, our observation provides a novel insight for the *Aloe* implication in microbicidal ability and skin immunity. *Aloe* treatment also induced the expression of molecules involved in several aspects of keratinocyte proliferation and differentiation such as **GRP78**, **Prohibitin**, and **Stathmin**. Prohibitin is a potential tumor suppressor protein that exhibits growth suppressor ability by repressing E2F-mediated gene transcription (Joshi *et al.*, 2003). Stathmin is a microtubule-destabilizing protein and, in association with Tubulin and HSP70, was reported to be functionally relevant in the control of numerous regulatory pathways that require a reorganization of the entire cytoskeleton. GRP78 (also known as HSRPA5) was found to be increased in the suprabasal layers of

normal epidermis and can work as a molecular chaperone in cooperation with other Heat Shock Proteins being part of the unfolded protein response activated in differentiating epidermal keratinocytes (Sugiura *et al*., 2009). In *Aloe*-treated HaCaT cells, heat shock proteins, essential for the survival of malignant cells, were under-represented. However, heat-shock proteins also occur under non-stressful conditions, simply 'monitoring' the cell's recycling or folding. Further experiments are needed to clarify this phenomenon.

Remarkably, Calmodulin and Keratin 1 signals were detected only in the control sample and disappeared following the *Aloe* treatment. The remaining proteins exhibited a sensitive decrement in the *Aloe*-treated sample.

CONCLUSIONS

The results presented in this study indicate a clear antiproliferative effect of an Aloe extract on several tumor cells and a prodifferentiative effect both on primary and immortalized human keratinocytes.

For a medicinal application perspective, our study supports the use of *Aloe arborescens* extract for topic treatment of hyperproliferative skin diseases or skin SCC. *In vivo* animal experimentation will be necessary to further confirm the proposed health benefit of the extract.

Acknowledgements

This work was funded by MIUR (PRIN 2009KFS94X_003) to V. Calabrò. This work was also supported by Aloe-Beta-HDR sas Capriati a Volturno - ITALY.

Conflict of Interest

The authors declare no conflict of interest.

REFERENCES

Arunkumar S, Muthuselvam M. 2009. Analysis of phytochemical constituents and antimicrobial activities of Aloe vera L. against Clinical Pathogens. *World J Agric Sci* **5**(5): 572–576.

Baccigalupi L, Di Donato A, Parlato M, *et al*. 2005. Small surface-associated factors mediate adhesion of a food-isolated strain of Lactobacillus fermentum to Caco-2 cells. *Res Microbiol* **156**: 830–8365

Bedini C, Caccia R, Triggiani D, Mazzucato A, Soressi GP, Tiezzi A. 2009. Micropropagation of Aloe arborescens Mill: A step towards efficient production of its valuable leaf extracts showing antiproliferative activity on murine myeloma cells. *Plant Biosystems-an Int J Deal Aspects Plant Biol* **143**(2): 233–240.

Di Costanzo A, Festa L, Duverger O, *et al*. 2009. Homeodomain protein Dlx3 induces phosphorylation-dependent p63 degradation. *Cell Cycle* **8**(8): 1185–95.

Di Cunto F, Topley G, Calautti E, *et al*. 1998. Inhibitory function of p21Cip/Waf1 in differentiation of primary mouse keratinocytes independent of cell cycle control. *Science* **280**: 1069–72.

Dotto P. 1999. Signal Transduction Pathway controlling the switch between keratinocyte growth and differentiation. *Crit Rev Oral Biol Med* **10**: 442–457

Fakhry S, Manzo N, D'Apuzzo E, *et al*. 2009. Characterization of intestinal bacteria tightly bound to the human ileal epithelium. *Res Microbiol* **160**(10): 817–823.

Greathead H. 2003. Plants and plants extracts for improving animal productivity. *Proc Nutr Soc* **62**: 279–290

Hochstrasser DF, Patchornik A, Merril CR. 1988. Development of polyacrylamide gels that improve the separation of proteins and their detection by silver staining. *Anal Biochem* **173**(2): 412–23.

Infascelli F, Tudisco R, Mastellone V, *et al*. 2010. Diet Aloe supplementation in pregnant buffalo cows improves colostrum immunoglobulin content. *Revista Veterinaria* **21**(Suppl. 1): 151–153.

Joshi B, Ko D, Ordonez-Ercan D, Chellappan SP. 2003. A putative coiled-coil domain of prohibitin is sufficient to repress E2F1-mediated transcription and induce apoptosis. *Biochem Biophys Res Commun* **312**(2): 459–6.

Laemmli UK. 1970. Cleavage of structural proteins during the assembly of the head of bacteriophage T4. *Nature* **227**: 680–685.

Lefort K, Mandinova A, Ostano P, *et al*. 2007. Notch1 is a p53 target gene involved in human keratinocyte tumor suppression through negative regulation of ROCK1/2 and MRCKα kinases. *Genes Dev* **21**: 562–577.

Lissoni P, Rovelli F, Brivio F, *et al*. 2009 A randomized study of chemotherapy versus biochemotherapy with chemotherapy plus Aloe arborescens in patients with metastatic cancer. *In Vivo* **23**(1): 171–5.

Naclerio G, Ricca E, Sacco M, De Felice M. 1993. Antimicrobial activity of a newly identified bacteriocin of B. cereus. *Appl Environ Microbiol* **59**: 4313–4316.

Niyonsaba F, Suzuki A, Ushio H, Nagaoka I, Ogawa H, Okumura K. 2009. The human antimicrobial peptide dermicin activates normal human keratinocytes. *Br J Dermatol* **160**(2): 243–249.

Paramio JM, Jorcano JL. 1997. Role of protein kinases in the in vitro differentiation of human epidermal HaCaT cells. *Br J Dermatol* **137**(1): 44–50.

Pecere T, Gazzola V, Mucignat C, *et al*. 2000. Aloe-emodin is a new type of anticancer agent with selective activity against neuroectodermal tumors. *Cancer Res* **60**: 2800–2804.

Rocco JW, Leong CO, Kuperwasser N, DeYoung MP, Ellisen LW. 2006. p63 mediates survival in squamous cell carcinoma by suppression of p73-dependent apoptosis. *Cancer Cell* **9**(1): 45–56.

Sugiura K, Muro Y, Futamura K, *et al*. 2009. The unfolded protein response is activated in differentiating epidermal keratinocytes. *J Invest Dermatol* **129**(9): 2126–35.

Vivo M, Di Costanzo A, Fortugno P, Pollice A, Calabrò V, La Mantia G. 2009. Downregulation of ΔNp63α in keratinocytes by p14ARF-mediated SUMO-conjugation and degradation. *Cell Cycle* **31**: 8(21): 3537–3543.

Wessel D, Flugge UI. 1984. A method for the quantitative recovery of protein in dilute solution in the presence of detergents and lipids. *Anal Biochem* **138**(1): 141–143.

Youngman P, Perkins JB, Sandman K. 1984. New genetic methods, molecular cloning strategies and gene fusion techniques for /Bacillus subtilis/ which take advantage of Tn/917/ insertional mutagenesis. In Hoch JA, Ganesan AT (eds.). Genetics and Biotechnology of Bacilli. Academic Press: NY; 103–111.

